PIV measurements of the effect of pulsed blowing jet on a NACA0012 wing model

José Hermenegildo García Ortiz[1], Jorge Aguilar Cabello [2], Alicia Guzmán Gómez [2], Luis Parras and Carlos del Pino[2*]

1: Dept. of Mechanical Engineering and Industrial Design, University of Cádiz, Spain

2: Dept. of Mechanical, Thermal and , The University of Málaga, Spain

* Correspondent author: cpino@uma.es

Keywords: 2D-PIV, aerodynamics, Active Control

ABSTRACT

Wingtip vortices are present in taking off and landing operations and their presence in airport runways must be reduced. To that end, several strategies have been considered in the last decades, being the active control one possible technical solution. To compute the effectiveness of active control that corresponds to pulsed low-blowing-ratio transverse jet for the reduction of the wingtip vortex strength, we carry out 2D-PIV measurements in a towing tank for chord-based Reynolds numbers $15 \cdot 10^3$ and $20 \cdot 10^3$. We consider two cases: (i) no active control $R_{jet} = 0$ and (ii) pulsating radial jet of blowing-ratio R_{jet} smaller than 1.7 (or momentum coefficient C_μ lower than 0.12) and different Strouhal numbers ranging from 0.27 to 0.94. Our observations show that the best reduction of wingtip vortex strength takes place at the lowest Strouhal number tested. We use the maximum azimuthal velocity and vorticity together with the circulation to quantify this decrease in the vortex strength. Besides, we define the spatial evolution of a disturbance parameter ξ which allow us to detect again the optimal frequency that leads to vortex destruction.

1. Introduction

The study of vortices appears in different engineering applications such as helicopters blades, propellers or aircraft wings. Concerning rotorcraft, there are also many interesting flow phenomena that arise from complex interactional aerodynamics for both hovering and forward flight. Many of these examples include blade vortex interactions, vortex pairing, vortex

breakdown, vortex-wake interactions and also the interaction between vortices and the fuselage. They can adversely affect rotorcraft aeromechanic and aeroacoustic performance in a significant number of applications. Furthermore, the case of propellers, the so-called tip vortex cavitation widely present within blades at high rotational speeds so that it is considered, among others the first experimental observation of cavitation that appears on ships or boats. Cavitation is an important phenomenon to take into account for propeller design whose requirements are low noise and vibration levels as reported in Pennings et al. (2015).

Nowadays, airport management regarding the aircraft traffic is still one of the main goal to be optimized because airports increase the number of passengers year by year. For this reason, there is a demand to reduce the time between consecutive landing and takeoff operations. The primary hazard present in airport runways are trailing vortices, so their strength must be reduced as much as possible. To achieve this objective, different active control strategies have been tested, see for instance Margaris and Gursul (2006, 2010). We sum up below relevant investigations on this issue.

The techniques that affect the vortex through forcing by an actuator are defined as Active Control. Some methods account for wingtip blowing, synthetics jet and morphed wings, among others. Blowing was the first technique and the most studied by researchers, probably due to its easier implementation. The most straightforward approach was the use of spanwise blowing in an attempt to increase the effective span. Ayers and Wilde (1956) were the first to describe the application of this blowing scheme to lift modulation and performed measurements on a swept wing and observed significant gains in the lift as well as a beneficial effect on the stall. Carefoli (1964) formulated a theory and conducted experiments with a straight wing and found that the main reason for lift gain is a virtual wing enlargement caused by the jet. Later, Carafoli and Camarasescu (1971) reported measurements on small-aspect-ratio wings, observing that lift augmentation is more intense for smaller aspect ratios, further suggesting that the primary mechanism for lift increment is an effective enlargement of the wingspan. More experimental work on lateral blowing was carried out by White (1963), who noticed some beneficial effects on drag under certain conditions. Wu et al. (1982) gave details of a tip blowing arrangement with several thin jets coming from slots whose length was a fraction of the wing chord. Although this procedure was not designed to extend the effective wingspan, it exhibited some similarities to the winglet concept.

A study of the vortex structure of the flow field associated with the type of tip blowing considered in our research has been reported by Tavella et al. (1986). These studies indicated that, for a tip jet whose chord is comparable to the wing chord, the wingtip vortex would usually engulf the vortices produced by the jet in cross-flow, with the result that in most cases only one

vortex was found downstream of the wingtip. Conversely, and using this tip blowing discrete jets, Wu et al. (1983) suggested that the complex vortex structure of a non-symmetric jet in cross-flow was preserved.

Later, Tavella et al. (1988) developed a theoretical study based on the same concept of lateral blowing and carried out experiments using a standard wing profile, NACA0018 with spanwise direction slot. As a result, it was found that the lift gain due to lateral blowing depends on the 2/3 power of the jet blowing intensity. Lee et al. (1989) modified the wing profile using several tip jet configurations giving rise to a multiple-vortex structure. In particular, secondary vortices (SV) in the near-field. An analysis of the near-field structure in such of the cases indicated that the presence of high SV provided the mechanism for the breakdown scaling laws. More recently, Zhou et al. (2004) measured the near-field of tip vortices ($x/c \leq 5$) with spanwise blowing as a means to modifying vortex growth. They managed to reduce the rotational momentum of the tip vortex using a high-speed jet blowing at the core of the tip vortex. For example, the maximum streamwise vorticity was halved by a jet velocity of about $10W_\infty$ where W_∞ is the free-stream velocity.

Margaris and Gursul (2010) analyzed the effect of continuous jet blowing at the tip vortex on the growth in the near-wake using the different wingtip-jet configurations. It was found that the high aspect ratio jet produces a pair of counter-rotating vortices of different strength; their interaction with the tip vortex leads to single or multiple-vortex wakes. The blowing from near the pressure surface resulted in diffused vortices in the near wake whereas blowing from near the suction surface produces the opposite effect. The tip shape was also varied; the round tip showed the ability to promote the Coanda effect, thus modifying the vortex interaction. The wing incidence was found to affect not only the tip vortex but also the jet-generated vortices.

2. Experimental setup

Experimental tests were conducted in a towing tank located in the laboratory of Aero-hydrodynamic at the University of Málaga (see a 3D layout in Fig. 1). The main reason for the use of a towing tank is the absence of elements that move the fluid and turbulence levels achieved are extremely small (less than 1%). The NACA0012 wing model (1) has a chord of 100 mm and a length of 200 mm of wingspan. This wing model has one orifice through the spanwise direction that allow us to blow a pulsating jet in the radial direction (negative y- axis in Fig. 1).

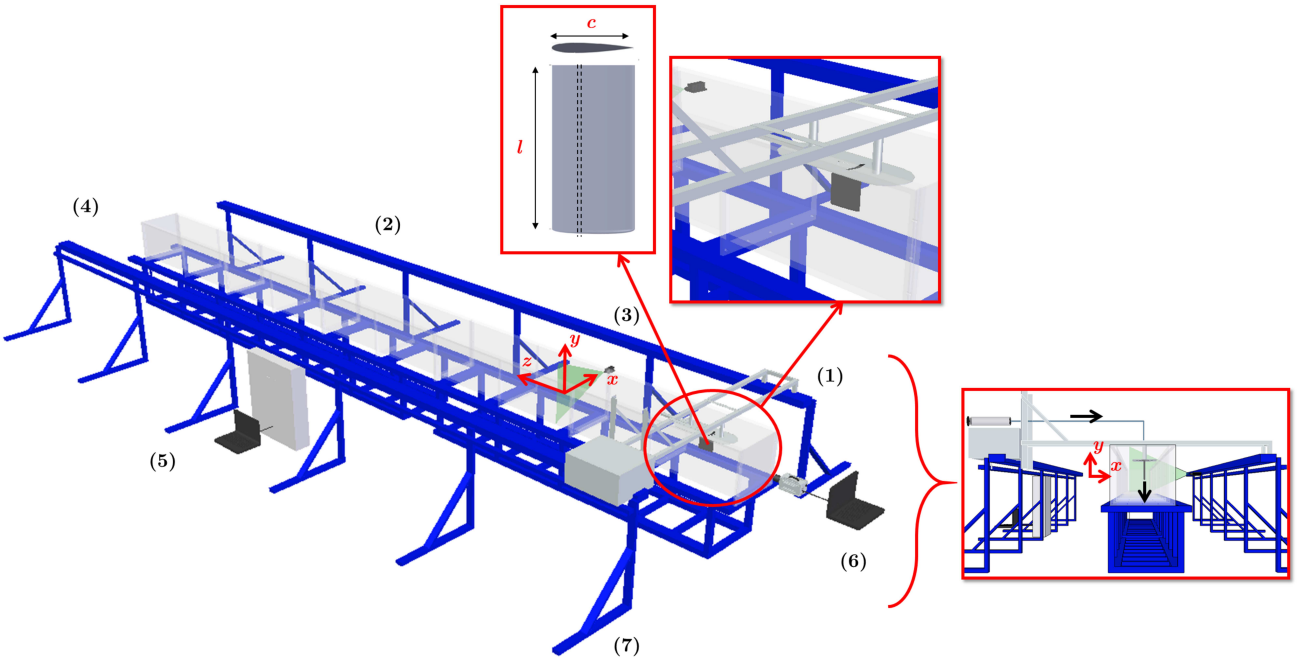

Fig. 1 Detail of the NACA0012 wing model in the experimental setup. Inset on the right focus on the injection system while the inset on the top corresponds to the wing model geometry and its mounting.

The NACA0012 wing model is pushed using a guide rail (2) in a towing tank that has 10 m long, and 0.5 × 0.5 m^2 cross-section, in perspex of 25 mm thickness (3) in order to allow for optical visualizations, as well as for 2D-PIV (6) measurements of the velocity field. The water in the tank is at rest and the wind model moves through it. The wing model is vertically assembled on the guide rail (2) that moves (from right to left in the schematic) through the whole towing tank. This guide was designed to achieve versatility for several experimental conditions (no control or active control). Besides, not only the wing model but also different types of equipment could be moved such as the camera, lasers (4) or pumps to carry out several tests. The towing tank used two rails which were made of iron (5). They were mounted with 90 degrees to bear the weight of the water and to guarantee the correct alignment within $\pm 0.1^o$. Also, all the iron structure (9) is aligned using a digital inclinometer within $\pm 0.1^o$. We imposed a constant velocity to the wing model. To that end, it has been installed an electric motor which provides a velocity between 1 and 1000 mm/s with an error lower than 0.5%. The electric motor is controlled by a laptop with feedback control by means of an encoder and the control of the acceleration from rest and the final position of the model was set using Matlab® through the USB port (6). The support allows different attack angles between the upstream flow and the wing model. In addition, the water temperature was measured by an equipment that consists of nine sensors in three groups along the towing tank. Each group had three sensors at different heights in the tank, so the average

temperature was measured along the tunnel. The sampling rate is a measure per second in each sensor obtaining an accuracy of $\pm 0.1^{o}C$.

We used one two dimensional Particle Image Velocimetry (2D-PIV) system for measuring the velocity field of the flapping plate. The 2D-PIV system consists of three components: (i) a laser sheet (less than 1 mm thick in the measurement section) obtained by means of three 0.5Wgreen laser sources (532 nm) in conjunction with a set of lenses (cylindrical lens of -6.25 mm focal length), (ii) a high speed camera model FASTCAM SA-3 which records images up to 60000 fps, with an internal memory of 4 GB, and a Nikon 60 mm lens (model AF Micro Nikkon 60mm) and f/2.8, and finally (iii) a synchronizer. Only a maximum frame rate of 125 fps was required for this experimental work. The PIV algorithm employed was DPIVSoft which performs a double pass PIV method with window deformation of 32x32 px, being the time step between images the inverse of the frame rate. Data reduction algorithms provide the true particle displacement and 2D velocity vector field at the illuminated plane, see Meunier and Leweke (2003).

Non-dimensional variables to describe the flow are defined as

$$\bar{r} = \frac{r}{c}, \bar{z} = \frac{z}{c}, \bar{v} = \frac{v}{W_{\infty}}, \overline{w} = \frac{w}{W_{\infty}}, \tag{1}$$

where Re_c is the Reynolds number based on the wing chord c defined as

$$Re_c = \frac{W_{\infty} c}{\nu}, \tag{2}$$

being ν the kinematic viscosity which is temperature dependent. Finally, the aspect ratio of the jet R_{jet} is defined as the outlet radial jet over the free-stream velocity. Firstly, and for the case of no blowing, $R_{jet} = 0$.

In flow control studies by blowing injection, we must define the jet-to-crossflow blowing ratio as

$$R_{jet} = \frac{W_{jet}}{W_{\infty}}, \tag{3}$$

where W_{jet} corresponds to the injection velocity. R_{jet} has a constant value for each Reynolds number because neither W_{∞} or W_{jet} change while doing one experimental test. We consider to

study in this work the influence of the jet frequency. The R_{jet} values for each Reynolds number correspond of R_{jet} =1.7 and 1.3 for chord based Reynolds numbers $15 \cdot 10^3$ and $20 \cdot 10^3$.

As mentioned above, two experiments were carried out to each different frequencies of the blowing jet and two Reynolds numbers. The synthetic jet was characterized using the momentum coefficient C_μ as defined by Amitay et al. (2001)

$$C_\mu = \frac{\overline{I_J}}{\frac{1}{2}\rho_0 W_\infty^2 c}, \tag{4}$$

in which ρ_0 is the free-stream fluid density, c is the chord, and $\overline{I_J}$ is the time-averaged jet momentum per unit length during the outstroke

$$\overline{I_J} = \frac{2}{T}\rho_j b \int_0^{T/2} u_j^2(t)dt\,, \tag{5}$$

where T is the period of the diaphragm motion, ρ_j is the jet density, b is the jet slot width and $u_j(t)$ is the phase-averaged velocity at the jet exit plane. Taking into account the characteristics of the blowing we are dealing in the present work, the momentum coefficient can be simplified as

$$C_\mu = \frac{2b}{c}\left(\frac{W_{jet}}{W_\infty}\right)^2, \tag{6}$$

which can be formulated in terms of the jet-to-crossflow blowing ratio R_{jet} as

$$C_\mu = \frac{2b}{c}R_{jet}^2\,, \tag{7}$$

In order to qualitatively evaluate the effect of the blowing on the vorticity structure along the axial coordinate z, a vorticity disturbance parameter ξ can be defined as

$$\xi = \frac{\int_\Omega (\omega_R - \omega_0)^2\, d\Omega}{\int_\Omega \omega_0^2\, d\Omega}, \tag{8}$$

where ω_0 and ω_R are the cross-sectional axial vorticity of the unperturbed ($R_{jet} = 0$) and the perturbed vortex, respectively. We integrate the vorticity in the cross-sectional area Ω. Remember that this parameter is equal to zero when no active control is applied while it should be near 1 when the active control has a strong effect, thus destroying the wingtip vortex (ω_R near zero).

Finally, the Strouhal numer is defined as

$$St = \frac{fc}{W_\infty}, \tag{9}$$

where f is the frequency of the pulsed blowing jet.

3. Experimental results

The 2D-PIV velocity field must be computed using the same frame, so the vortex core is known in each pair of images to avoid wandering effects, see more details in del Pino et al. (2011). For this reason, we re-center the vortex core in each frame using the minimum velocity or the maximum vorticity to detect the axis. Besides, it is interesting to know that the post-processing of raw PIV images could not be carried out for the largest axial coordinate in all the cases. More specifically, for the cases in which the presence of the pulsed blowing jet was present, the PIV code showed several errors that made impossible to continue with the 2D-PIV process. However, these errors are present for certain chords, usually from $\bar{z}$ ranging between 17 and 21, because the vortex disappears after applying the active control, so it was challenging to identify its core or even its vorticity. For the cases in which this fact occurs, post-processing has been stopped.

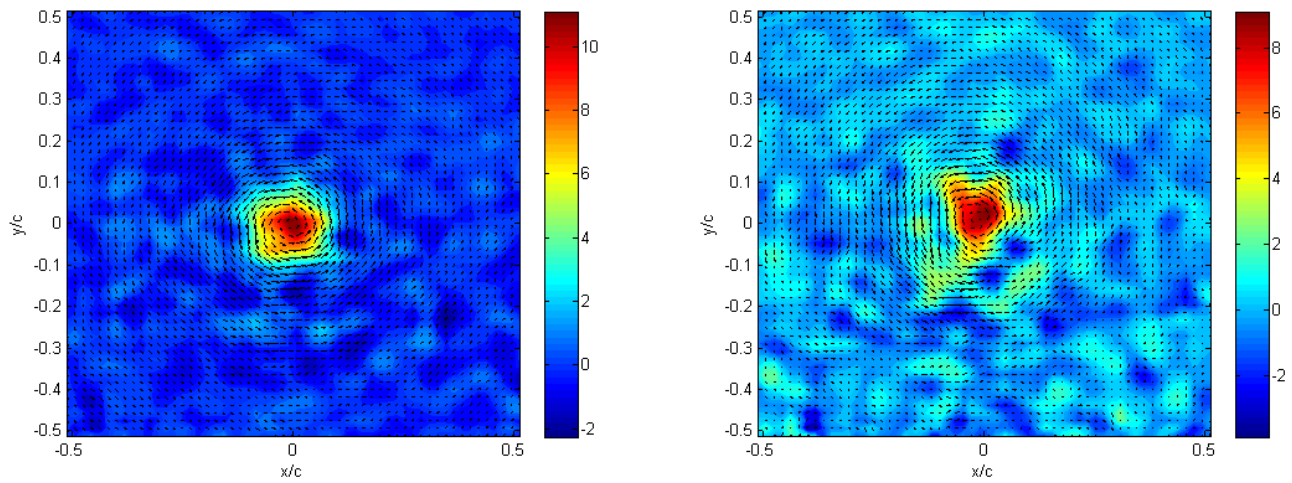

(a) (b)

Fig. 2 Comparison between of the non-dimensional vorticity between R_{jet}=0 (a) and R_{jet}=1.3 or C_μ=0.07 with St=0.27 (b) at $\bar{z}$=10 for Re_c= $20 \cdot 10^3$.

In Fig. 2 we present one example of the velocity field (vectors) with superimposed vorticity field for $Re_c = 20 \cdot 10^3$ and no-injection (a) and pulsating injection (b) using St=0.27. We observe a reduction in the maximum vorticity field when we apply the active control. Also, the vortex seems to be symmetric in the case of non-injection (a) in comparison to that of injection (b).

We carried out several experimental tests to compute the axial evolution in the stream direction of the maximum azimuthal velocity and vorticity up to 40 non-dimensional chords. We depict in Fig. 3 these two variables for different ratios of the pulsating blowing jet that correspond to different Strouhal numbers. It can be observed that these two magnitudes decrease with the axial coordinate. There is a significant reduction of the vortex strength for the lowest frequencies tested in both Reynolds numbers. In addition, and though the Reynolds number has been increased slightly from $Re_c = 15 \cdot 10^3$ to $Re_c = 20 \cdot 10^3$, there is a strong influence of the active control on Re_c since the vortex was destroyed for any Strouhal number in a smaller axial location for the lowest Reynolds number. This fact may be explained in terms of the increment of the momentum coefficient C_μ from 0.07 ($Re_c = 20 \cdot 10^3$) to 0.12 ($Re_c = 15 \cdot 10^3$).

Paying our attention to the circulation and the vorticity disturbance parameter ξ shown in Fig. 4, we observe that the circulation remains roughly constant, as expected, and their associated parameter ξ increase from 0 to 1. Note that some peak values of ξ greater than 1 are caused by the lack of accuracy while applying the 2D-PIV technique. The circulation is weakly affected by the pulsed blowing jet, see Figs. 4 (a) and (c). This means that the aerodynamic characteristics of the NACA0012 wing model are the same, so the lift force must not be influenced strongly after the application of the pulsed blowing jet. This is the desired effect after applying the active control. The scattered fluctuations presented in the circulation stems from the fact that the trailing vortex is almost destroyed, so the images to perform 2D-PIV are not accurate neither to detect the vortex core or the particles around it. The vorticity disturbance parameter ξ represents the influence on the vortex destruction, as it is depicted in Fig. 4 (b) and (d) for $Re_c = 15 \cdot 10^3$ and $Re_c = 20 \cdot 10^3$, respectively. It is shown that the lowest frequencies tested are the best candidates to enhance vortex diffusion because this disturbance parameter achieves values close to one rapidly.

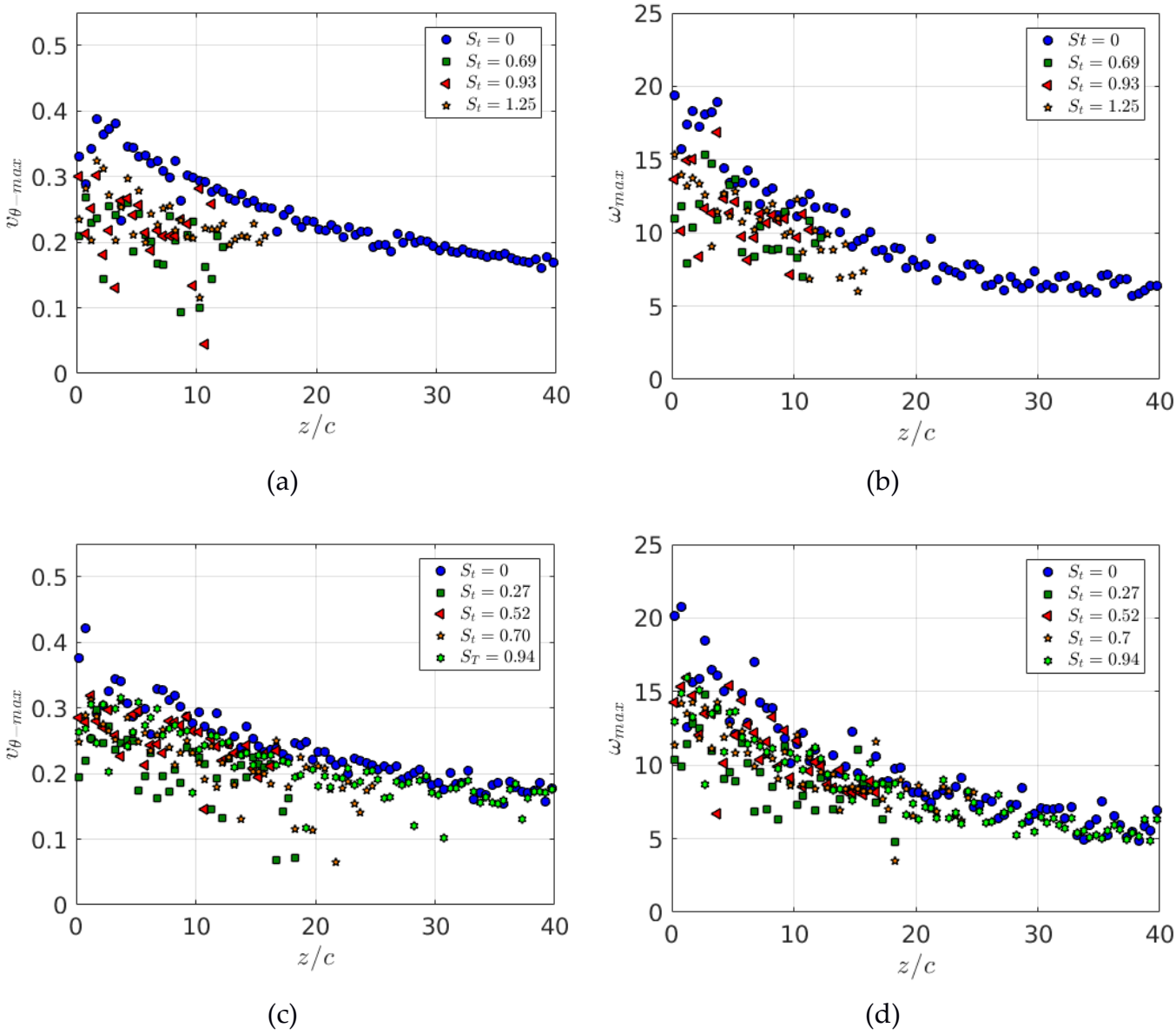

Fig. 3 Comparison between the non-dimensional magnitudes: maximum of azimuthal velocity (a)-(c), and maximum vorticity (b)-(d) for $Re_c = 15 \cdot 10^3$ and $Re_c = 20 \cdot 10^3$, respectively, and for several Strouhal numbers, as indicated in the legend.

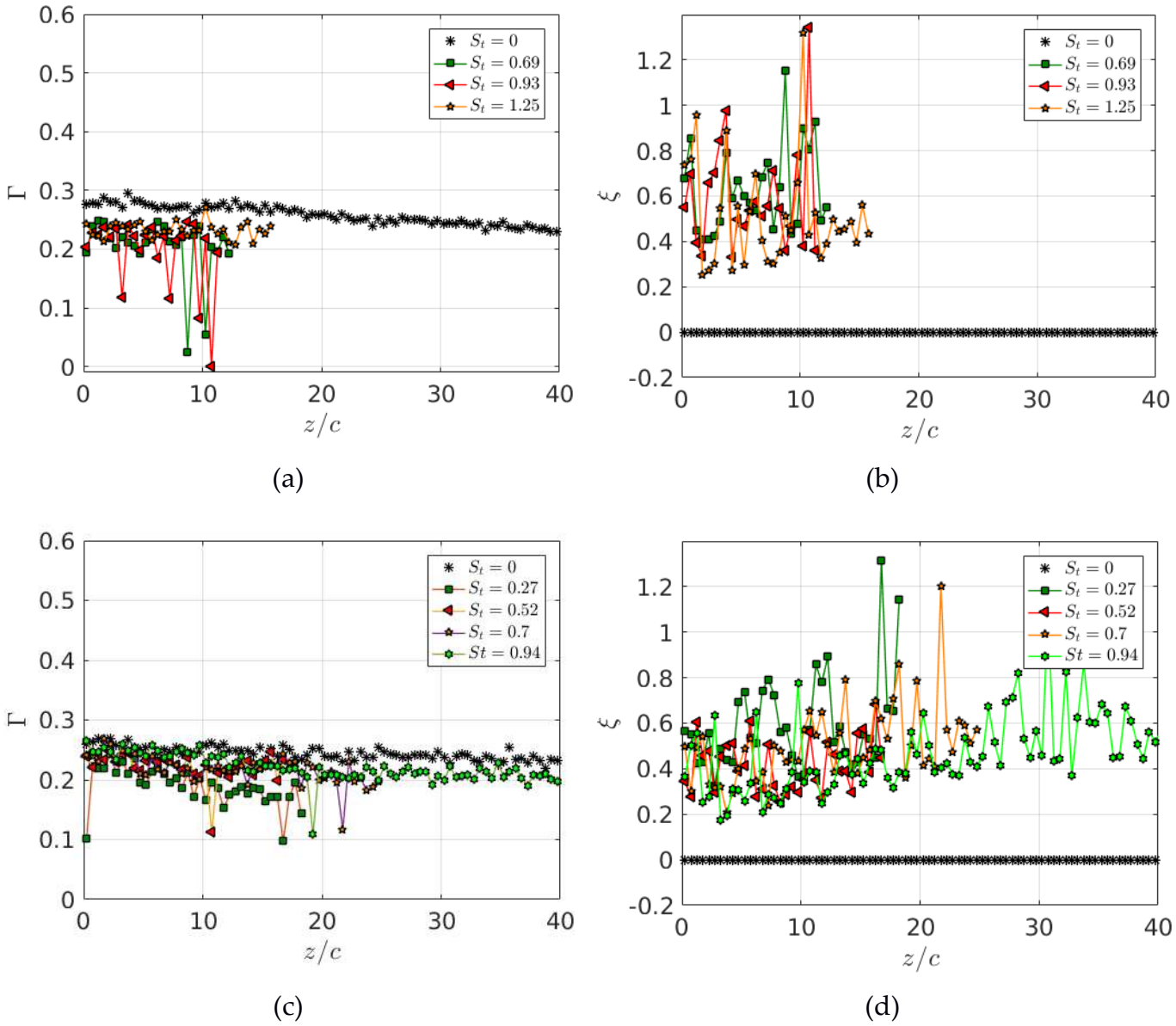

Fig. 4. Circulation (a)-(c) and disturbance parameter ξ (b)-(d) for $Re_c = 15 \cdot 10^3$ and for $Re_c = 20 \cdot 10^3$, respectively, and for several Strouhal numbers, as indicated in the legend.

4. Conclusions

We perform 2D-PIV to know the impact of active control using pulsed low blowing ratio transverse jet into the reduction of the wingtip vortex strength. Two chord-based Reynolds numbers $15 \cdot 10^3$ and $20 \cdot 10^3$ have been tested. We consider two cases: no active control $R_{jet} = 0$ and pulsating radial jet for blowing-ratio R_{jet} smaller than 1.7 (or momentum coefficient C_μ lower than 0.12). Different Strouhal numbers ranging from 0.27 to 0.94 have been also proved. Our observations show that the best reduction of wingtip vortex strength takes place at the lowest Strouhal number tested. We use the maximum azimuthal velocity and vorticity together with the circulation to quantify this decrease in the vortex strength. In addition, we define and present the spatial evolution of a disturbance parameter ξ that allow us to detect the optimal frequency again to enhance vortex diffusion. In all the cases, the active control has a weak influence on the circulation, so the lift coefficient must not be affected while applying the pulsed blowing jet.

We would like to compare 2D-PIV measurements with those obtained using 3D-PIV. This is a work in progress.

This work has been supported by the Ministerio de Economía y Competitividad (Spain) Grant No. DPI2013-40479-P and DPI2016-76151-C2-1-R and Junta de Andalucía Grant No. P11-TEP-7776.

References

Amitay, M and Smith, D R and Kibens, V and Parekh, D E and Glezer A (2001), Aerodynamic Flow Control over an Unconventional Airfoil Using Synthetic Jet Actuators, AIAA J 39 (3), 361-370

Ayers, R. F. and Wilde, M. R. (1956), Aerodynamic characteristics of a swept wing with spanwise blowing. An experimental investigation of the aerodynamic characteristics of a low aspect ratio swept wing with blowing in a spanwise direction from the tip, The college of Aeronautics Cranfield.

Carafoli, E (1964) The influence of lateral jets, simple or combined with longitudinal jets, upon the wing lifting characteristics, increased lift of wings of STOL aircraft by use of lateral fluid jets, simple or combined with longitudinal jets, Nasa Technical Reports Server.

Carafoli, E and Camarasescu, N (1971), New Researches on Small Span-Chord Ratio Wings with Lateral Jets, DTIC Document.

del Pino, C., Parras, L., Felli, M. y Fernandez-Feria, R.(2011), Structure of trailing vortices: Comparison between particle image velocimetry measurements and theoretical models. Physics of Fluids, 23, 113602.

Lee, C S and Tavella, D A and Wood, N J (1989), Flow structure and scaling laws in lateral wing tip blowing, AIAA Journal, 8 (27), 1002–1007.

Margaris, P and Gursul, I (2006), Wing tip vortex control using synthetic jets, The Areonautical Journal, 673-681.

Margaris, P and Gursul, I (2010), Vortex topology of wing tip blowing, Aerospace Science and Tecnlogy 14, 143 160.

Meunier, P and Leweke, T (2003) Analysis and optimization of the error caused by high velocity gradients in PIV. Exp. Fluids 35: 408–421.

Pennings, P C and Bosschers, J and Westerweel, J and van Terwisga, T J C (2015)., Dynamics of isolated vortex cavitation, Journal of Fluid Mechanics, 778, 288-313.

Tavella, D A and Lee, C S and Wood, N J (1986), Influence wing tip configuration on lateral blowing efficiency, 24thAerospace Sciences Meeting, American Institute of Aeronautics and Astronautics, Aerospace Sciences Meetings.

Tavella, D A and Wood, N J and Lee, C S and Roberts, L (1988), Lift modulation with lateral wing-tip blowing, Journal of Aircraft, 4 (25), 311-316.

White, H E (1963), Wind-Tunnel Investigation of the Use of Wing Tip Blowing to Reduce Drag for Take-Off and Landing, DTIC Document.

Wu, J M and Vakili, A and Chen, Z (1982), Wing-tip jets aerodynamics performance, ICAS 1982 Congress.

Wu, J and Vakili, A and Chen, Z and Gilliam, F (1983), Investigations on the effects of discrete wingtip jets, 21st Aerospace Sciences Meeting, American Institute of Aeronautics and Astronautics, Aerospace Sciences Meetings.

Zhou, Y and Zhang, H J and Whitelaw, J H (2004), Wing-Tip Vortex Measurement With Particle Image Velocimetry, 34h AIAA Applied Aerodynamics Conference.